



Throughput enhancement for millimeter wave communications using reconfigurable intelligent surfaces

Raed Alhamad¹ · Hatem Boujemaa²

Accepted: 13 November 2021 / Published online: 7 January 2022

© The Author(s), under exclusive licence to Springer Science+Business Media, LLC, part of Springer Nature 2021

Abstract

In this paper, we propose to extend the coverage of millimeter-wave (mmwave) communications using Reconfigurable Intelligent Surfaces (RIS). The first hop between the source and the relay node uses millimeter-wave communications. The received signal at relay node R is affected by P interferers. The relay node decodes the transmitted packet by the source. Then, the relay node transmits the decoded packet to the destination. A RIS is placed between relay R and destination D . RIS is implemented as a reflector to reflect signals from R to D . All reflected signals have the same phase so that the throughput is significantly enhanced. RIS is also implemented as a transmitter and illuminated with the antenna of relay node R . We show that RIS allows up 19, 25, 31, 37 dB gain with respect to conventional millimeter-wave communication without RIS for a number of reflectors $N = 16, 32, 64, 128$. We also propose RIS for mmwave communications using Non Orthogonal Multiple Access (NOMA). A set of RIS reflectors is dedicated to each NOMA user. The proposed NOMA system using RIS offers 10, 13, 16, 20, 24, 27 and 30 dB gain with respect to conventional NOMA using millimeter-wave communications without RIS for a number of reflector per user $N = N_1 = N_2 = 8, 16, 32, 64, 128, 256, 512$.

Keywords RIS · Millimeter-wave communications · Nakagami channels · Throughput analysis

1 Introduction

Millimeter wave communications (mmwave) have been suggested for future 6G networks to enhance the throughput of wireless communications and reach data rates of multiple Gb/s [1–3]. Millimeter-wave operates on a large bandwidth going from 30 to 300 GHz [5–7]. Relay nodes can be deployed to improve the throughput of millimeter-wave communications to benefit from cooperative diversity and improve the throughput [7–10]. However, relaying techniques are complex to implement and require orthogonal channels to avoid interference between relayed signals [7–10]. Using orthogonal channels will reduce the throughput and spectral efficiency. Another solution is to use relay selection techniques for millimeter-wave communications. Relay selection

techniques are complex to implement and require a central node to select the best relay. Relay selection techniques require extra-signalization to activate the relay and to send their SNRs to a central node. Besides, the number of relays is limited and cannot be around a hundred relays. Relaying consumes power at relay nodes and requires extra-processing.

To avoid these drawbacks, we suggest extending the coverage of millimeter-wave communications using RIS implemented as a reflector or a transmitter [11–15]. The link between source and relay node uses millimeter wave communications. The signals received at the relay node are affected by P interferers. The relay decodes the received packet and forwards it to the destination. RIS is placed between the relay node and destination. RIS contains a large number of reflectors $N = 16, 32, 64, 128$ with phase shifts optimized so that all N reflections have the same phase at the destination. The phase of k th reflector compensates the phase shift of channel gains between relay/ k th RIS reflector and k th RIS reflector/destination [16–20]. The receiver output at the destination is similar to that of a Maximum Ratio Combiner (MRC) with a number of branches equal to the number of reflectors N [20–24]. We propose a second implementation of RIS as a transmitter in which RIS is illuminated with the

✉ Raed Alhamad
ralhamad@seu.edu.sa

Hatem Boujemaa
boujemaa.hatem@supcom.tn

¹ Information Technology Department, Saudi Electronic University, Riyadh, Kingdom of Saudi Arabia

² COSIM-SUP'COM, Tunis, Tunisia

antenna of relay R . When RIS is implemented as a transmitter, the phase shift of k th RIS reflector depends on the phase of channel gain between relay node and destination. Some experimental results of RIS are discussed in [24].

Millimeter wave communications for NOMA systems using multiple antennas was suggested in [25,26]. User assisted cooperative relaying for millimeter wave communications using NOMA was proposed in [27]. The coverage probability of millimeter wave communication using NOMA was derived in [28]. Hybrid precoding/combining techniques for millimeter wave communications was suggested in [29]. Deep learning assisted calibrated beam training was used in [30] for millimeter wave communications. A high gain resonant cavity antenna was proposed in [31] to improve the performance of millimeter wave communications.

The contributions of the paper are:

- We suggest enhancing the throughput of millimeter wave communications using RIS. RIS is implemented as a reflector or a transmitter. We show that RIS allows up to 19, 25, 31, 37 dB gain with respect to conventional millimeter wave communication without RIS for a number of reflectors $N = 16, 32, 64, 128$.
- The use of RIS to extend the coverage of millimeter wave communications has not been yet proposed in [1–10]. Previous papers implemented multiple relay nodes for millimeter wave communications [1–10].
- We derive the throughput of millimeter wave communications using RIS as a reflector or a transmitter for Nakagami channels. We compare the obtained theoretical results to computer simulations.
- We study the performance of wireless communications using RIS in the presence of interferers. In previous papers, there is no interference on RIS link [11–24].
- The derived results evaluate the throughput at the packet level and are valid for any number of interferers at relay node and destination. Besides, the results are valid for any position of the source, relay node and RIS.
- We propose the use of RIS for mmwave communications using NOMA. The proposed NOMA system using RIS offers 10, 13, 16, 20, 24, 27 and 30 dB gain with respect to conventional NOMA using millimeter wave communications without RIS [25–28] for a number of reflector per user $N = N_1 = N_2 = 8, 16, 32, 64, 128, 256, 512$.

The paper contains five sections. The next section studies the millimeter wave and RIS links when there is a single destination. RIS has been implemented as a reflector or a transmitter to enhance the throughput at the destination. Section 3 extends the system model to NOMA systems. Section 4 provides some theoretical and computer simulation results. Conclusions and perspectives are provided in last section.

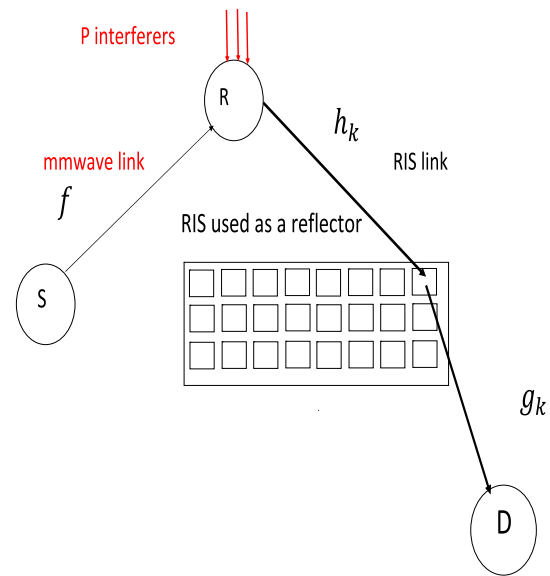


Fig. 1 RIS deployed as a reflector

2 Performance analysis of millimeter wave communications using RIS

2.1 Single destination

2.1.1 Millimeter wave link

The system model depicted in Fig. 1 is composed of a source S , a relay node R , and a destination D . We assume that the received signal at R is affected by P interferers. In interference-limited millimeter-wave communications, the SINR at R is equal to [1–5]

$$\Gamma_{SR,mmwave} = \frac{E_S |f|^2}{I} \tag{1}$$

in which E_S is the symbol energy S , f is the channel coefficient between S and R , I is the interference term at R composed of P interferers:

$$I = \sum_{q=1}^P E_q |i_q|^2 \tag{2}$$

in which E_q is the transmitted energy per symbol of q th interferer, i_q is the channel gain between q th interferer and R .

For Nakagami fading channels, $X = E_S |f|^2$ follows a Gamma distribution $Gamma(M, \beta)$ defined as

$$f_X(x) = \frac{x^{M-1} e^{-\frac{x}{\beta}}}{\Gamma(M)\beta^M} \tag{3}$$

$M > 0.5$ is the m-fading figure of Nakagami channel,

$$\beta = \frac{E_S E(|f|^2)}{M} \tag{4}$$

$E(\cdot)$ is the expectation operator.

The interference I at the relay node is expressed as

$$I = \sum_{q=1}^P I_q \tag{5}$$

in which $I_q = E_q |i_q|^2$

We assume that I is the sum of independent and identically distributed (i.i.d) Gamma random variables (r.v) I_q that follows a $\text{Gamma}(M, \alpha)$

$$\alpha = \frac{E(I_q)}{M} \tag{6}$$

The sum of P i.i.d Gamma r.v. I_q is a Gamma r.v. $G(PM, \alpha)$. We deduce that $\Gamma_{SR,m}$ is the quotient of two Gamma r.v. that has a general prime distribution and Probability Density Function (PDF) [32]:

$$f_{\Gamma_{SR,m}}(x) = \frac{\Gamma(M + PM)\alpha^M x^{M-1} \left(1 + \frac{x\alpha}{\beta}\right)^{-PM-M}}{\beta^M \Gamma(M)\Gamma(PM)} \tag{7}$$

in which subscript m refers to mmwave. The proof is provided in ‘‘Appendix 1’’.

We have [33]

$${}_2F_1(A, B; C; z) = \frac{\Gamma(C)}{\Gamma(B)\Gamma(C - B)} \times \int_0^1 x^{B-1} (1-x)^{C-B-1} (1-zx)^{-A} dx \tag{8}$$

in which $B > 0, C > 0, {}_2F_1(A, B; C; Z)$ is the hypergeometric function. We use (8) to write the Cumulative Distribution Function (CDF) of SINR as

$$F_{\Gamma_{SR,m}}(x) = {}_2F_1\left(PM + M, M; M + 1, \frac{-x\alpha}{\beta}\right) \times \frac{\Gamma(M + PM)(x\alpha)^M}{\Gamma(M)\Gamma(PM)\beta^M} \tag{9}$$

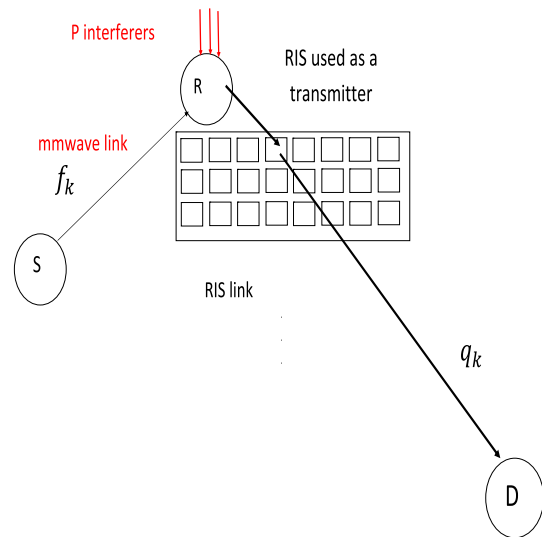


Fig. 2 RIS deployed as a transmitter

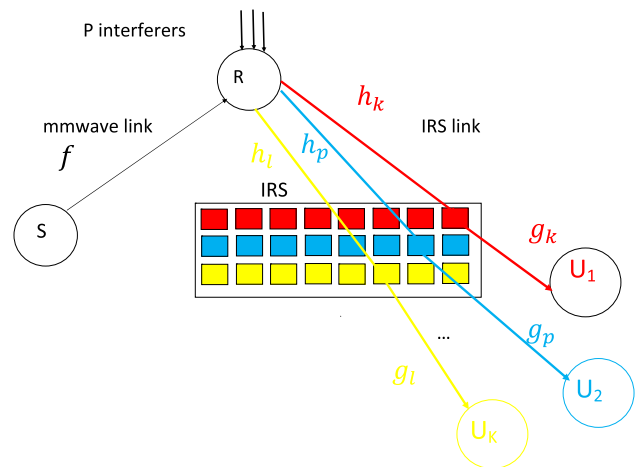


Fig. 3 Millimeter wave communications using RIS and NOMA

2.1.2 RIS link

2.1.2.1 RIS implemented as a reflector

To extend the coverage of millimeter-wave communications, a RIS is placed between relay node R and destination D . We define h_k as the channel coefficient between R and k th RIS reflector with average power $E(|h_k|^2) = \frac{1}{d_1^{PLE}}$ in which $E(\cdot)$ is the expectation operator, PLE is the path loss exponent and d_1 is the distance between R and RIS. We define g_k as the channel coefficient between k th reflector of RIS and destination D with average power $E(|g_k|^2) = \frac{1}{d_2^{PLE}}$ in which d_2 is the distance between RIS and D . RIS are nearly-passive devices with very low complexity [11] made of electromagnetic material that can be deployed on several structures including but not limited to building facades, walls... Therefore, the use of RIS does not increase too much

the overall computational complexity of the proposed system [11].

Let a_k and b_k be the absolute value and phase of $h_k = a_k e^{-j b_k}$. For Nakagami channels, a_k has a Gamma distribution with $E(a_k) = \frac{\Gamma(M+0.5)}{\Gamma(M)} \sqrt{\frac{1}{M d_1^{PLE}}}$ and $E(a_k^2) = E(|h_k|^2) = \frac{1}{d_1^{PLE}}$ [34]. Let c_k and d_k be the absolute and phase of $g_k = c_k e^{-j d_k}$. We have $E(c_k) = \frac{\Gamma(M+0.5)}{\Gamma(M)} \sqrt{\frac{1}{M d_2^{PLE}}}$ and $E(c_k^2) = E(|g_k|^2) = \frac{1}{d_2^{PLE}}$ [34].

RIS optimizes the phase ϕ_k of k th reflector as follows

$$\phi_k = b_k + d_k. \tag{10}$$

During p th symbol period, the received signal at D is equal to

$$r_p = s_p \sqrt{E_R} \sum_{q=1}^N h_q g_q e^{j \phi_q} + n_p \tag{11}$$

in which N is the number of RIS reflectors, s_p is the p th transmitted symbol, n_p is zero-mean Gaussian r.v. with variance N_0 and E_R is the symbol energy of R .

Using (9–10), we obtain

$$r_p = \sqrt{E_R} s_p A + n_p, \tag{12}$$

in which

$$A = \sum_{q=1}^N a_q c_q. \tag{13}$$

where $a_q = |h_q|$ and $c_q = |g_q|$.

The Signal to Noise Ratio (SNR) at D is expressed as

$$\Gamma_{RD,r} = \frac{E_R A^2}{N_0}. \tag{14}$$

in which subscript r refers to RIS.

a_q and $a_{q'}$ are assumed to be independent for $q \neq q'$ as they correspond to channel coefficient between R and q th, q' th RIS reflector. c_q and $c_{q'}$ are assumed to be independent for $q \neq q'$ as they correspond to channel coefficient between q th, q' th RIS reflector and destination. a_q and $c_{q'}$ are assumed to be independent $\forall q \neq q'$ as they correspond to channel coefficient of different links (relay to RIS and RIS to destination). Therefore, $a_q c_q$ and $a_{q'} c_{q'}$ are independent $q \neq q'$. Using the Central Limit Theorem (CLT), A can be approximated

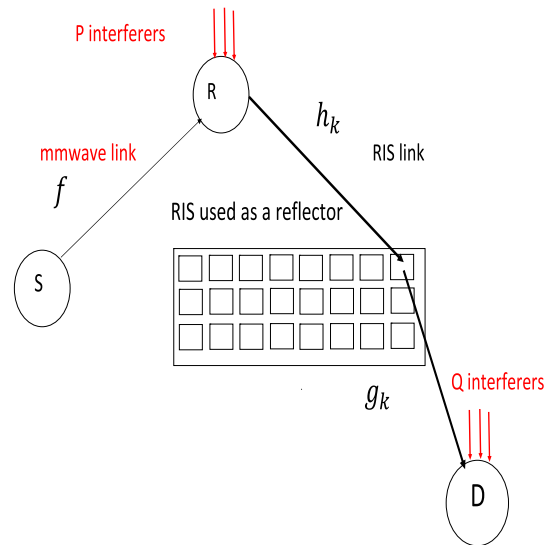


Fig. 4 RIS deployed as a reflector in the presence of Q interferers at D

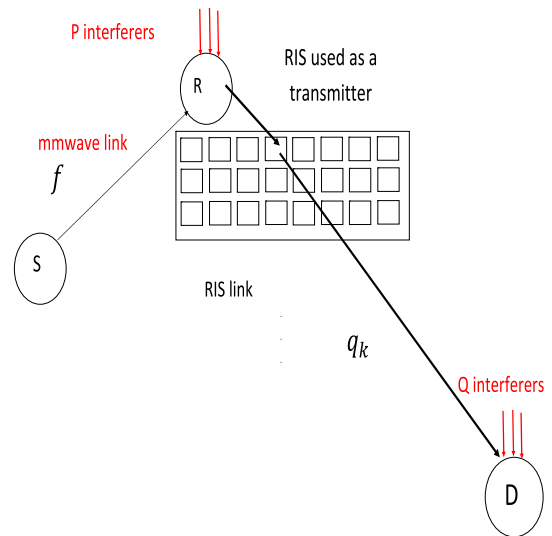


Fig. 5 RIS deployed as a transmitter in the presence of Q interferers at D

by a Gaussian r.v. with mean $m_A = \frac{N \Gamma(M+0.5)^2}{M \Gamma(M)^2 d_1^{PLE/2} d_2^{PLE/2}}$ and variance $\sigma_A^2 = \frac{N}{d_2^{PLE} d_1^{PLE}} [1 - \frac{\Gamma(M+0.5)^4}{M^2 \Gamma(M)^4}]$.

To obtain the values of m_A and σ_A^2 , we used the following results for Nakagami channels with fading figure M [34]: $E(a_k^2) = \frac{1}{d_1^{PLE}} = \Omega_1$ and $E(a_k^n) = \frac{\Gamma(M+0.5n)}{\Gamma(M)} (\frac{\Omega_1}{M})^{0.5n} \forall n \geq 1$. We deduce $E(a_k) = \frac{\Gamma(M+0.5)}{\sqrt{M \Gamma(M)} d_1^{PLE/2}}$. Similarly, we have $E(c_k^2) = \frac{1}{d_2^{PLE}}$ and $E(c_k) = \frac{\Gamma(M+0.5)}{\sqrt{M \Gamma(M)} d_2^{PLE/2}}$. As a_q and c_q are independent, we deduce $m_A = \sum_{q=1}^N E(a_q c_q) = N E(a_q) E(c_q) = N \frac{\Gamma(M+0.5)^2}{M \Gamma(M)^2 d_1^{PLE/2} d_2^{PLE/2}}$.

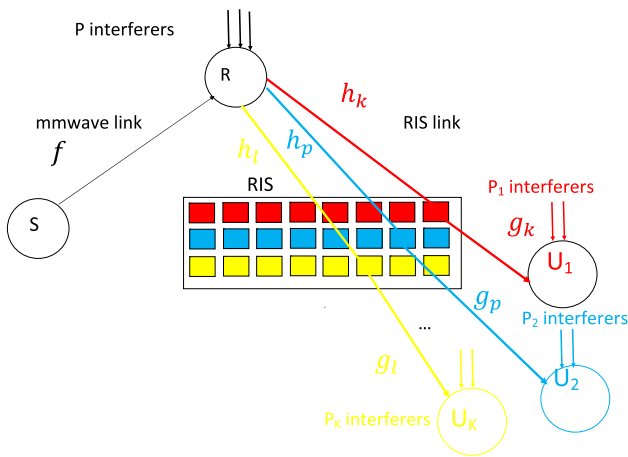
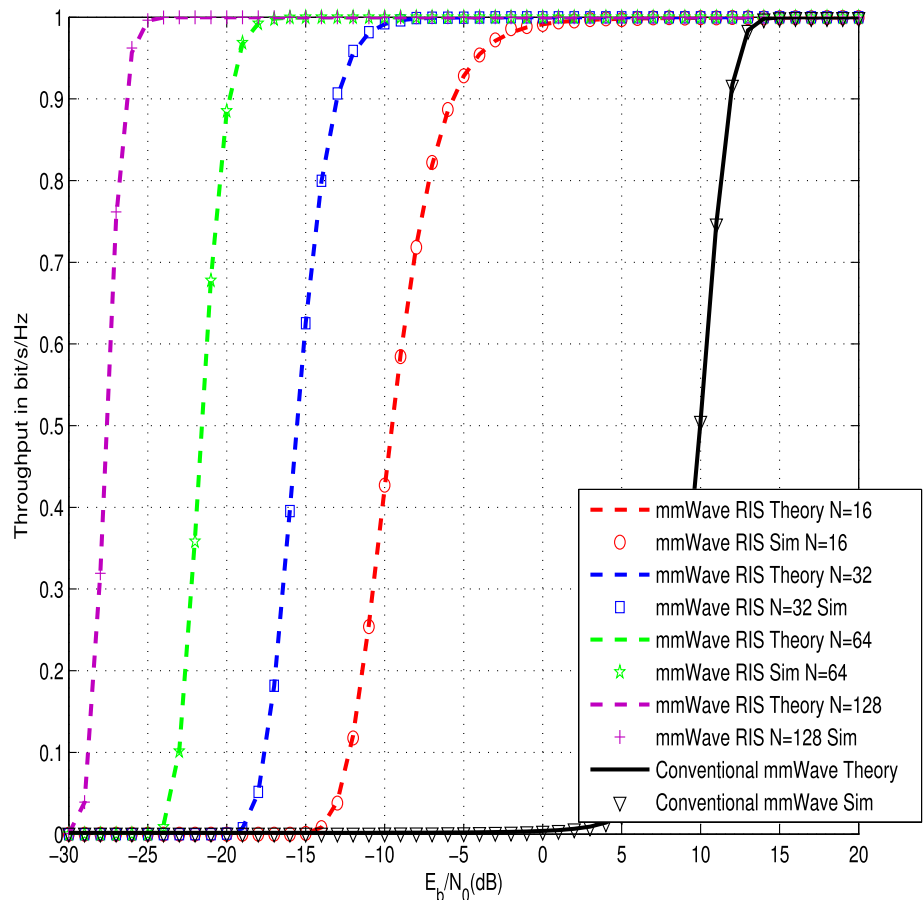


Fig. 6 Millimeter wave communications using RIS in the presence of P_i interferers at user U_i

Since $a_q c_q$ and $a_{q'} c_{q'}$ are independent $q \neq q'$, $Var(A) = \sigma_A^2 = \sum_{q=1}^N Var(a_q c_q) = N Var(a_q c_q) = N[E(a_q^2 c_q^2) - E(a_q c_q)^2]$. Since a_q and c_q are independent, we obtain $Var(A) = N[E(a_q^2)E(c_q^2) - E(a_q)^2 E(c_q)^2] = N[\frac{1}{d_1^{PLE} d_2^{PLE}} - \frac{\Gamma(M+0.5)^4}{M^2 \Gamma(M)^4 d_1^{PLE} d_2^{PLE}}]$

Fig. 7 Throughput of mmWave using RIS as a reflector: QPSK modulation



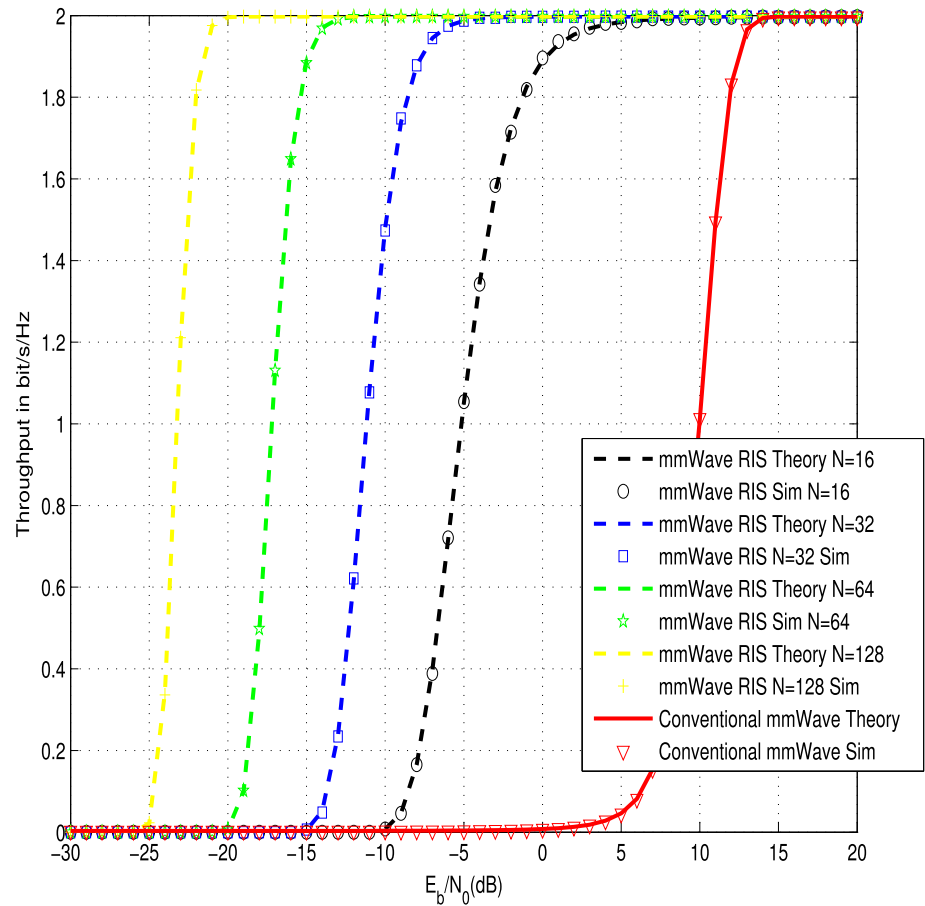
The CDF of SNR at D is written as

$$F_{\Gamma_{RD,r}}(x) = P\left(\frac{E_R A^2}{N_0} \leq x\right) = P\left(-\sqrt{\frac{x N_0}{E_R}} \leq A \leq \sqrt{\frac{x N_0}{E_R}}\right) \approx 0.5 \operatorname{erfc}\left(\frac{-\sqrt{\frac{x N_0}{E_R}} - m_A}{\sqrt{2} \sigma_A}\right) - 0.5 \operatorname{erfc}\left(\frac{\sqrt{\frac{x N_0}{E_R}} - m_A}{\sqrt{2} \sigma_A}\right) \quad (15)$$

2.1.2.2 RIS implemented as a transmitter

In Fig. 2, a RIS is placed at relay R . As explained in section V of [11], RIS can be deployed as a transmitter at relay node R . It is used as a transmitter and illuminated with an antenna of R . We define q_k as the channel gain between RIS and destination D . Let e_k and ζ_k be the absolute value and phase of $q_k = e_k e^{-j\zeta_k}$. For Nakagami channels, e_k is Gamma distributed with mean $E(e_k) = \frac{\Gamma(M+0.5)}{\Gamma(M)} \sqrt{\frac{1}{M d_3^{PLE}}}$ [34] and average power $E(e_k^2) = E(|q_k|^2) = \frac{1}{d_3^{PLE}}$ in which d_3 is the distance between relay R and D . RIS can be implemented

Fig. 8 Throughput of mmWave using RIS as a reflector: 16QAM modulation, weak turbulence



using Q Phase Shift Keying (PSK) modulation. Let μ_k be the phase of k th reflector of RIS:

$$\mu_k = \zeta_k + z_m, \tag{16}$$

in which $z_m = \frac{2\pi(n-1)}{M}$ is the phase of PSK symbol.

The received signal at D is written as

$$r_p = \sqrt{E_R} \sum_{l=1}^N q_l e^{j\mu_l} + n_k = \sqrt{E_R} e^{jz_m} \sum_{l=1}^N e_l + n_p, \tag{17}$$

The SNR at D is expressed as

$$\Gamma_{RD,r} = \frac{E_R B^2}{N_0}, \tag{18}$$

in which subscript r refers to RIS and

$$B = \sum_{l=1}^N e_l. \tag{19}$$

e_l and $e_{l'}$ are independent $\forall l \neq l'$ as they correspond to absolute value of channel coefficient between l th, l' th RIS reflector and destination. Using the CLT, B is approximated by a Gaussian r.v. with mean $m_B = N \frac{\Gamma(M+0.5)}{\Gamma(M)\sqrt{Md_3^{PLE}}}$ and

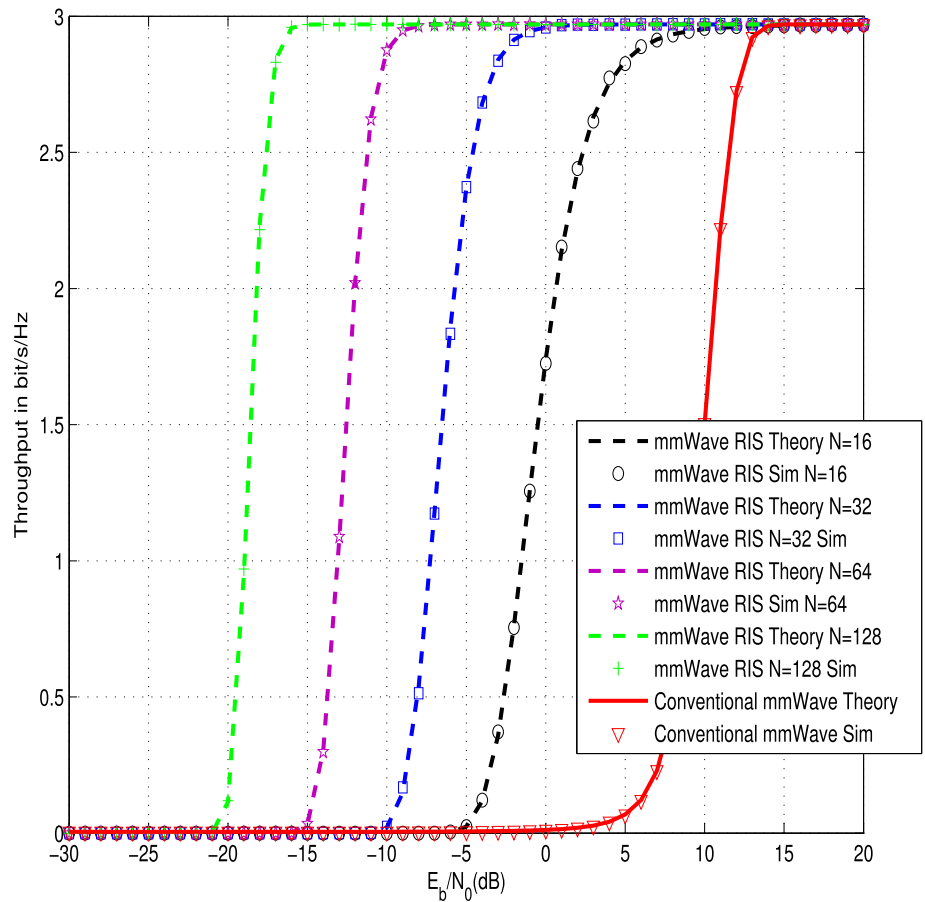
variance $\sigma_B^2 = \frac{N(1 - \frac{\Gamma(M+0.5)^2}{\Gamma(M)^2 M})}{d_3^{PLE}}$, d_3 is the distance between R equipped with RIS and D .

We use [34] $E(e_l) = \frac{\Gamma(M+0.5)}{\sqrt{M}\Gamma(M)d_3^{PLE/2}}$ to compute $m_B = \sum_{l=1}^N E(e_l) = N \frac{\Gamma(M+0.5)}{\sqrt{M}\Gamma(M)d_3^{PLE/2}}$. Since e_l and $e_{l'}$ are independent $\forall l \neq l'$, we deduce $\sigma_B^2 = \sum_{l=1}^N Var(e_l) = N Var(e_l) = N[E(e_l^2) - E(e_l)^2] = N[\frac{1}{d_3^{PLE}} - \frac{\Gamma(M+0.5)^2}{M\Gamma(M)^2 d_3^{PLE}}]$.

The CDF of SNR is given by

$$\begin{aligned} F_{\Gamma_{RD,r}(x)} &= P\left(\frac{E_R B^2}{N_0} \leq x\right) = P\left(-\sqrt{\frac{xN_0}{E_R}} \leq B \leq \sqrt{\frac{xN_0}{E_R}}\right) \\ &\simeq 0.5 \operatorname{erfc}\left(\frac{-\sqrt{\frac{xN_0}{E_R}} - m_B}{\sqrt{2}\sigma_B}\right) - 0.5 \operatorname{erfc}\left(\frac{\sqrt{\frac{xN_0}{E_R}} - m_B}{\sqrt{2}\sigma_B}\right) \end{aligned} \tag{20}$$

Fig. 9 Throughput of mmWave using RIS as a reflector: 64QAM modulation



2.2 RIS for mmwave communications using NOMA

2.2.1 Millimeter wave link

The system model of Fig. 3 shows a source S , a relay R and K NOMA users $U_i, i = 1, \dots, K$. U_i is the i th strong user. The source transmits a combination of K symbols $s_i, i = 1, 2, \dots, K$ dedicated to K users:

$$s = \sqrt{E_S} \sum_{i=1}^K \sqrt{H_i} s_i \tag{21}$$

in which $0 < H_i < 1$ is the fraction of power allocated to user U_i . More power is allocated to the weak user: $0 < H_1 < H_2 < \dots < H_K$. We have

$$\sum_{i=1}^K H_i = 1. \tag{22}$$

It is assumed that the received signal at relay node R is affected by P interferers: [1–5]

$$r = fs + I = f \left[\sqrt{E_S} \sum_{i=1}^K \sqrt{H_i} s_i \right] + I. \tag{23}$$

in which f is the channel coefficient between S and R , I is the interference term at R :

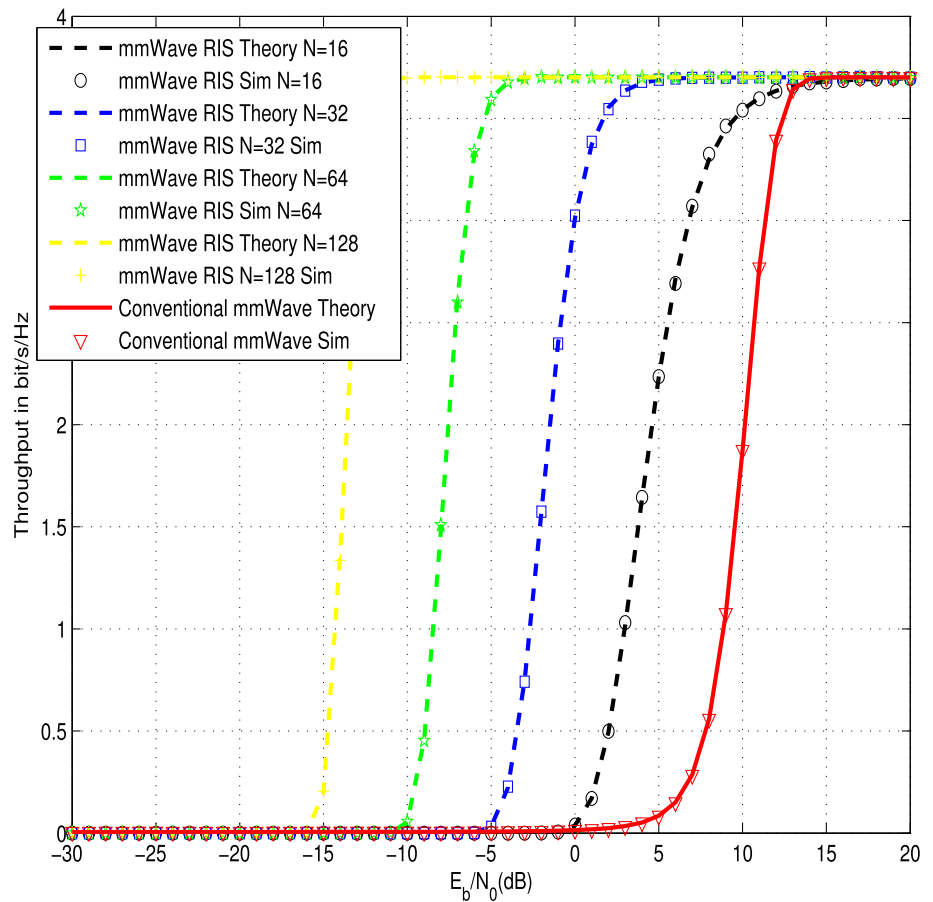
$$I = \sum_{q=1}^P E_q |i_q|^2 \tag{24}$$

E_q is the TES of q th interferer, i_q is the channel coefficient between q th interferer and R .

Relay node detects the symbol of user U_K since $H_K > H_i$. The SINR is given by

$$\Gamma_{R,K} = \frac{H_K E_S |f|^2}{I + E_S |f|^2 \sum_{i=1}^{K-1} H_i} \tag{25}$$

Fig. 10 Throughput of mmWave using RIS as a reflector: 256QAM modulation



Then, relay R removes the contribution of s_K and detects s_{K-1} with SINR

$$\Gamma_{R,K-1} = \frac{H_{K-1}E_S|f|^2}{I + E_S|f|^2 \sum_{i=1}^{K-2} H_i} \tag{26}$$

R will detect s_p $p = K, K - 1, \dots, 1$ with SINR

$$\Gamma_{R,p} = \frac{H_p E_S |f|^2}{I + E_S |f|^2 \sum_{i=1}^{p-1} H_i} \tag{27}$$

The Cumulative Distribution Function (CDF) of $\Gamma_{R,p}$ is given by

$$\begin{aligned} F_{\Gamma_{R,p}(x)} &= P\left(\frac{H_p E_S |f|^2}{I + E_S |f|^2 \sum_{i=1}^{p-1} H_i} \leq x\right) \\ &= P\left(\frac{H_p U}{1 + U \sum_{i=1}^{p-1} H_i} \leq x\right) \\ &= F_{\Gamma_{SR,m}}\left(\frac{x}{H_p - x \sum_{i=1}^{p-1} H_i}\right) \end{aligned} \tag{28}$$

in which $F_{\Gamma_{SR,m}}(x)$ is the CDF of $\Gamma_{SR,m}$ (9).

There is no outage at R when SINR $\Gamma_{R,1}, \Gamma_{R,2}, \dots, \Gamma_{R,K}$ are higher than x :

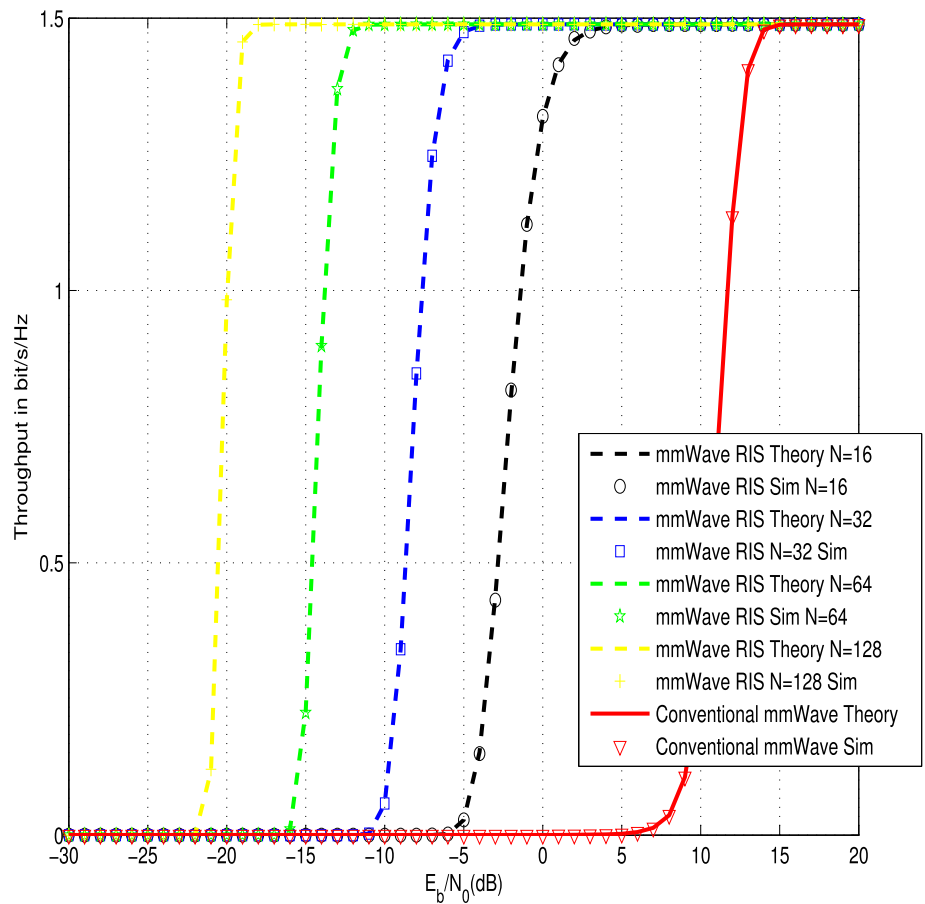
$$\begin{aligned} P_{\text{outage},R}(x) &= 1 - P(\Gamma_{R,1} > x, \dots, \Gamma_{R,K} > x) \\ &= F_{\Gamma_{SR,m}}\left(\max_{1 \leq p \leq K} \left(\frac{x}{H_p - x \sum_{i=1}^{p-1} H_i}\right)\right) \end{aligned} \tag{29}$$

2.2.2 RIS link

RIS is located between relay node R and users U_1, U_2, \dots, U_K . In Fig. 5, the red (respectively blue and yellow) reflectors are dedicated to user U_1 (respectively U_2 and U_K). A set O_i of reflectors are dedicated to user U_i . We define h_k as the channel coefficient between R and k th RIS reflector such that $E(|h_k|^2) = \frac{1}{D^{pLE}}$ and D is the distance between R and RIS. We define $g_k \in O_i$ as the channel coefficient between k th reflector of RIS and user U_i such that $E(|g_k|^2) = \frac{1}{D_i^{pLE}}$, D_i is the distance between RIS and U_i . O_i is the set of RIS reflectors dedicated to user U_i .

Let a_k and b_k be the absolute value and phase of $h_k = a_k e^{-jb_k}$. For Nakagami channels, a_k has a Gamma dis-

Fig. 11 Throughput of mmWave using RIS as a transmitter: 8PSK modulation



tribution with $E(a_k) = \frac{\Gamma(M+0.5)}{\Gamma(M)} \sqrt{\frac{1}{MD^{PLE}}}$ and $E(a_k^2) = E(|h_k|^2) = \frac{1}{D^{PLE}}$ [34]. Let c_k and d_k be the absolute and phase of $g_k = c_k e^{-jd_k}$. We have $E(c_k) = \frac{\Gamma(M+0.5)}{\Gamma(M)} \sqrt{\frac{1}{MD_i^{PLE}}}$ and $E(c_k^2) = E(|g_k|^2) = \frac{1}{D_i^{PLE}}$ [34].

RIS uses the following phase ϕ_k of k th reflector

$$\phi_k = b_k + d_k. \tag{30}$$

The received signal at U_i is written as

$$r = S\sqrt{E_R} \sum_{q \in O_i} h_q g_q e^{j\phi_q} + n \tag{31}$$

in which O_i is the set of reflectors dedicated to U_i , S is the transmitted NOMA symbol by relay node R , n is zero-mean Gaussian r.v. with variance N_0 and E_R is the TES of R .

Let \hat{s}_i the i th detected symbol at relay node R . When the detection is successful at the relay $\hat{s}_i = s_i$. The transmitted NOMA symbol S by relay R is written as

$$S = \sum_{l=1}^K \sqrt{G_l} \hat{s}_l \tag{32}$$

G_l is the fraction of power dedicated at U_l at relay R . More power is dedicated to weak user: $0 < G_1 < G_2 < \dots < G_K$. We have $\sum_{l=1}^K G_l = 1$.

Using (31–32), we have

$$r = \sqrt{E_R} \left[\sum_{l=1}^K \sqrt{G_l} \hat{s}_l \right] \sum_{q \in O_i} h_q g_q e^{j\phi_q} + n \tag{33}$$

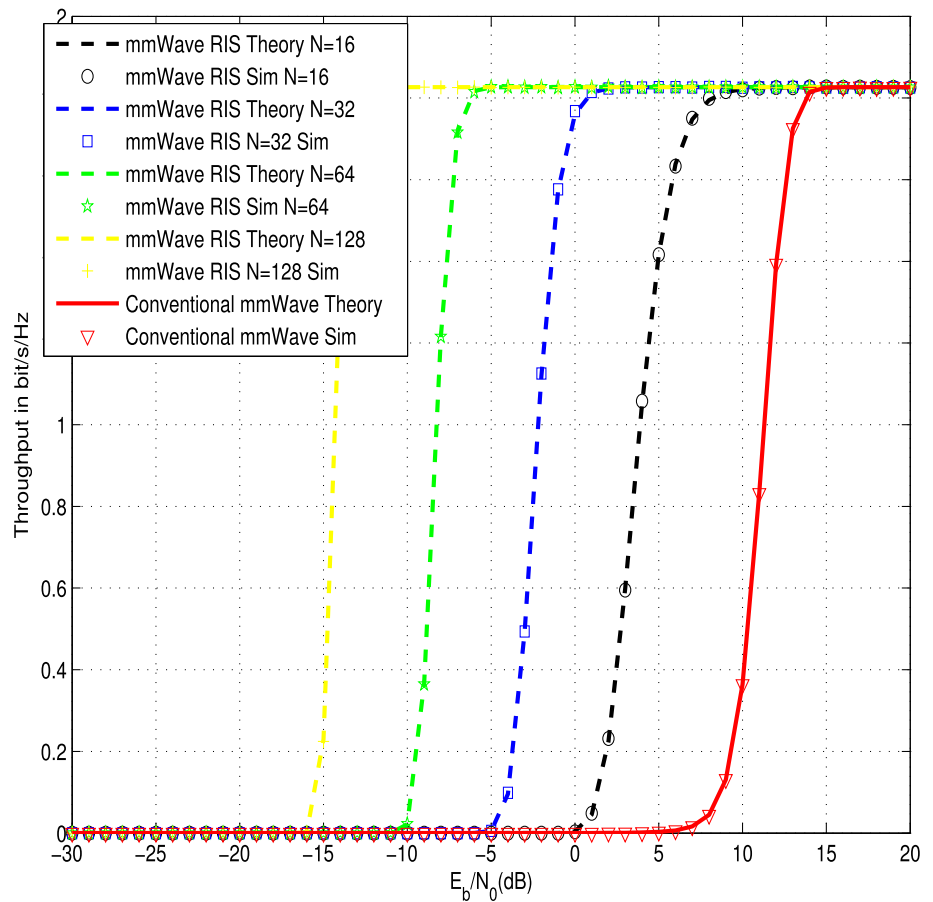
Using (30), we obtain

$$r = \sqrt{E_R} A_i \left[\sum_{l=1}^K \sqrt{G_l} \hat{s}_l \right] + n, \tag{34}$$

in which

$$A_i = \sum_{q \in O_i} a_q c_q. \tag{35}$$

Fig. 12 Throughput of mmWave using RIS as a transmitter: 16PSK



Using the Central Limit Theorem (CLT), A_i can be approximated by a Gaussian r.v. with mean $m_{A_i} = \frac{N_i \Gamma(M+0.5)^2}{M \Gamma(M)^2 d^{PLE/2} d_i^{PLE/2}}$ and variance $\sigma_{A_i}^2 = \frac{N_i}{d^{PLE} d_i^{PLE}} [1 - \frac{\Gamma(M+0.5)^4}{M^2 \Gamma(M)^4}]$, $N_i = |O_i|$ is the number of RIS reflectors dedicated to U_i .
The CDF of A_i^2 is written as

$$F_{A_i^2}(x) = P(A_i^2 \leq x) = P(-\sqrt{x} \leq A_i \leq \sqrt{x})$$

$$\simeq 0.5 \operatorname{erfc}\left(\frac{-\sqrt{x} - m_{A_i}}{\sqrt{2}\sigma_{A_i}}\right) - 0.5 \operatorname{erfc}\left(\frac{\sqrt{x} - m_{A_i}}{\sqrt{2}\sigma_{A_i}}\right) \quad (36)$$

User U_i detects first the symbol of user U_K as $G_K > G_i$ $\forall i \neq K$ with SINR

$$\Gamma_{U_i,K} = \frac{E_R A_i^2 G_K}{N_0 + E_R A_i^2 \sum_{l=1}^{K-1} G_l} \quad (37)$$

User U_i removes the signal of U_K using SIC and detect the symbol of U_{K-1} with SINR

$$\Gamma_{U_i,K-1} = \frac{E_R A_i^2 G_{K-1}}{N_0 + E_R A_i^2 \sum_{l=1}^{K-2} G_l} \quad (38)$$

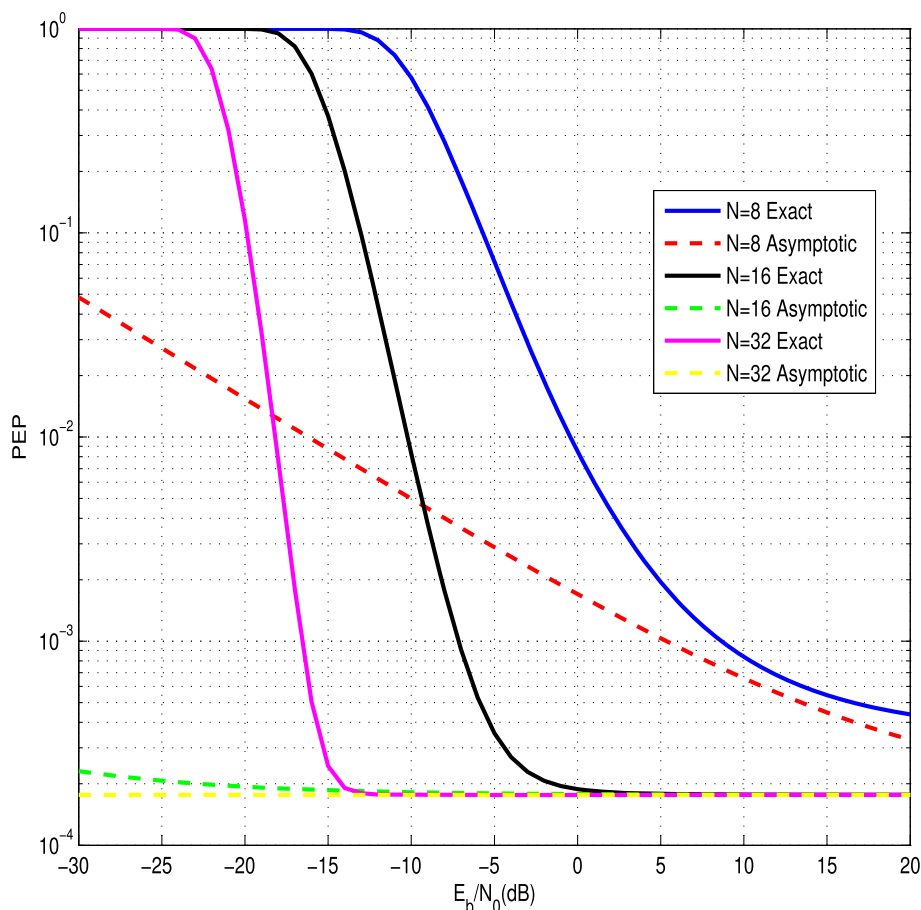
User U_i detects the symbols of users U_p $p = K, K-1, \dots, i$ with SINR

$$\Gamma_{U_i,p} = \frac{E_R A_i^2 G_p}{N_0 + E_R A_i^2 \sum_{l=1}^{p-1} G_l} \quad (39)$$

There is no outage at U_i when all SINR are larger than x :

$$P_{\text{outage},U_i}(x) = 1 - P(\Gamma_{U_i,K} > x, \Gamma_{U_i,K-1} > x, \dots, \Gamma_{U_i,i} > x) = F_{A_i^2}\left(\max_{i \leq p \leq K} \left(\frac{N_0 x}{E_R G_p - x E_R \sum_{l=1}^{p-1} G_l}\right)\right) \quad (40)$$

Fig. 13 Exact and asymptotic PEP using RIS as a reflector: QPSK



3 Throughput analysis in the presence of interferers

3.1 RIS link analysis in the presence of interferers and a single destination

Figures 4 and 5 depict the system model in the presence of Q interferers at the destination. The SINR at D is expressed as

$$\Gamma_{RD,r} = \frac{E_R C^2}{N_0 + J} \tag{41}$$

in which $C = A$ (13) when RIS is implemented as a reflector, $C = B$ (19) when RIS is implemented as a transmitter and J is the interference at D expressed as

$$J = \sum_{q=1}^Q J_q \tag{42}$$

$J_q = E'_q |j_q|^2$, E'_q is the transmitted energy per symbol of q th interferer and j_q is the channel coefficient between q th interferer and D . J_q are assumed to be i.i.d so that the J

follows a Gamma distribution $\text{Gamma}(QM, \zeta)$ written as

$$f_{J(y)} = \frac{y^{QM-1} e^{-\frac{y}{\zeta}}}{\Gamma(MQ)\zeta^{MQ}} \tag{43}$$

in which $\zeta = \frac{E(J_q)}{M}$.

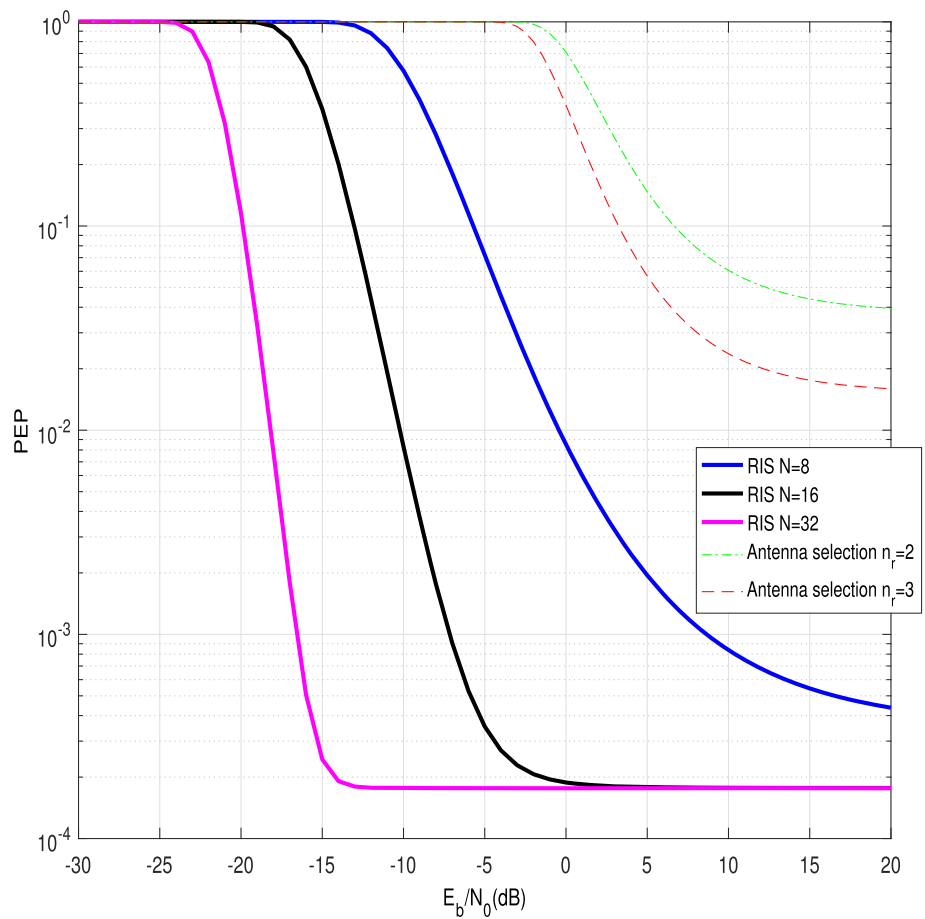
In the presence of Q interferers at D , the CDF of SNR is computed numerically as follows

$$F_{\Gamma_{RD,r}(x)} = \int_0^{+\infty} P(E_R C^2 \leq (N_0 + y)x) f_J(y) dy \tag{44}$$

in which $P(E_R C^2 \leq (N_0 + y)x)$ is written as (15) and (20) by replacing x by $(N_0 + y)x$ and N_0 by 1:

$$P(E_R C^2 \leq (N_0 + y)x) \simeq 0.5 \operatorname{erfc} \left(\frac{-\sqrt{\frac{(N_0+y)x}{E_R}} - m_C}{\sqrt{2}\sigma_C} \right) - 0.5 \operatorname{erfc} \left(\frac{\sqrt{\frac{(N_0+y)x}{E_R}} - m_C}{\sqrt{2}\sigma_C} \right) \tag{45}$$

Fig. 14 PEP using RIS or antenna selection at the destination: QPSK



$m_C = m_A, \sigma_C = \sigma_A$ when RIS is implemented as a reflector and $m_C = m_B, \sigma_C = \sigma_B$ when RIS is implemented as a transmitter.

3.2 Throughput analysis in the presence of a single destination

To avoid an outage at D , we should not have an outage on millimeter wave and RIS links. Therefore, the outage probability at D is written as

$$P_{\text{outage},m,r(x)} = 1 - [1 - F_{\Gamma_{SR,m}}(x)][1 - F_{\Gamma_{RD,r}}(x)] \quad (46)$$

in which subscript m, r refers to a system where the first hop uses conventional mmwave communications while the second one uses RIS.

When RIS is used as a reflector and at a high average SNR of RIS link, the asymptotic CDF is given by

$$F_{\Gamma_{SR,m}}(x) \approx \sqrt{\frac{N_0 2x}{\pi E_R}} \frac{e^{-\frac{m_A^2}{2\sigma_A^2}}}{\sigma_A} \quad (47)$$

When RIS is used as a transmitter and at a high average SNR of RIS link, the asymptotic CDF is given by

$$F_{\Gamma_{SR,m}}(x) \approx \sqrt{\frac{N_0 2x}{\pi E_R}} \frac{e^{-\frac{m_B^2}{2\sigma_B^2}}}{\sigma_B} \quad (48)$$

The asymptotic CDF is proportional to $\sqrt{\frac{N_0}{E_R}}$. It decays exponentially in N and can be minimized by increasing the number of reflectors N . Using (46-48), we can deduce the asymptotic outage probability.

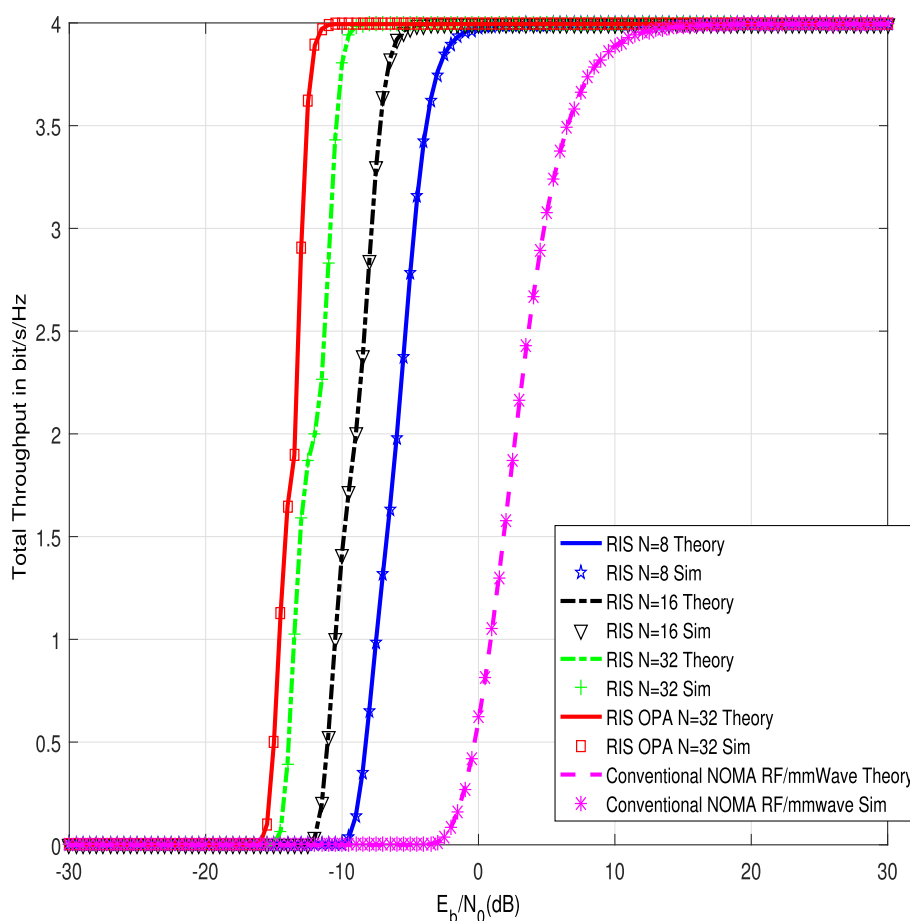
The Packet Error Probability (PEP) at D is upper bounded by the outage probability taken at waterfall threshold W_{TH} [35]

$$PEP_D < P_{\text{outage},m,r}(W_{TH}) \quad (49)$$

in which W_{TH} is a waterfall threshold defined as [35]

$$W_{TH} = \int_0^{+\infty} \text{PEP}(y) dy, \quad (50)$$

Fig. 15 Total throughput for 16QAM modulation : : 2 users



For Quadrature Amplitude Modulation of size Q , $PEP(y)$ is defined as

$$PEP(y) = 1 - [1 - 2 \left(1 - \frac{1}{\sqrt{Q}}\right) \operatorname{erfc}\left(\sqrt{\frac{3y}{Q-1}}\right)]^L \quad (51)$$

For PSK modulation of size Q , $PEP(y)$ is defined as

$$\operatorname{pep}(y) = 1 - [1 - \operatorname{erfc}\left(\sqrt{y \sin^2\left(\frac{\pi}{Q}\right)}\right)]^L \quad (52)$$

in which L is packet length in symbols.

To compute the PEP in (51), we used equation (7) of [28] where the left term is the PEP and the right term is the outage probability at W_{TH} .

Using (49 and 50), we can deduce the asymptotic PEP. The throughput at D is evaluated as

$$\operatorname{Thr}_D = 0.5 \log_2(Q) [1 - \operatorname{PEP}_D] \quad (53)$$

3.3 RIS link analysis in the presence of P_i interferers at NOMA user U_i

Figure 6 depicts the system model in the presence of P_i interferers user U_i . User U_i detects the symbols of users U_p $p = K, K - 1, \dots, i$ with SINR

$$\Gamma_{U_i,p} = \frac{E_R A_i^2 G_p}{N_0 + J_i + E_R A_i^2 \sum_{l=1}^{p-1} G_l} \quad (54)$$

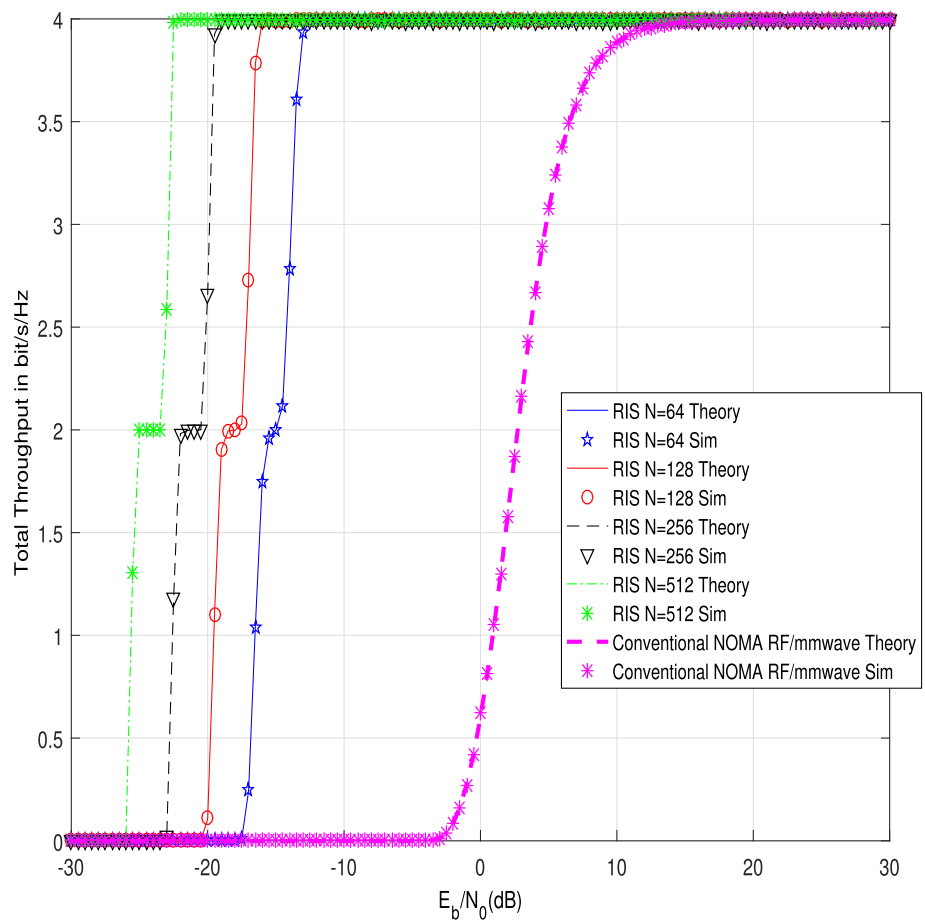
in which J_i is the interference at U_i expressed as

$$J_i = \sum_{q=1}^{P_i} J_{i,q} \quad (55)$$

$J_q = E'_q |j_q|^2$, E'_q is the TES of q th interferer and j_q is the channel coefficient between q th interferer and D . J_q are assumed to be i.i.d so that the J_i follows a Gamma distribution $\operatorname{Gamma}(P_i M, \zeta_i)$ written as

$$f_{J_i}(y) = \frac{y^{P_i M - 1} e^{-\frac{y}{\zeta_i}}}{\Gamma(M P_i) \zeta_i^{M P_i}} \quad (56)$$

Fig. 16 Total throughput for 16QAM modulation: : $N = 64, 128, 256, 512$



in which $\zeta_i = \frac{E(J_{i,q})}{M}$.

In the presence of P_i interferers at U_i , the outage probability at U_i is computed numerically as follows

$$P_{\text{outage},U_i}(x) = \int_0^{+\infty} F_{A_i^2} \left(\max_{1 \leq p \leq K} \left(\frac{(N_0 + y)x}{E_R G_p - x E_R \sum_{l=1}^{p-1} G_l} \right) \right) f_{J_i}(y) dy, \tag{57}$$

in which $f_{J_i}(y)$ is the PDF of interference at U_i (56) and $F_{A_i^2}(x)$ is provided in (36).

3.4 Throughput optimization in the presence of K NOMA users

The end-to-end (e2e) outage probability at user U_i is given by

$$P_{\text{outage},e2e,U_i}(x) = 1 - [1 - P_{\text{outage},U_i}(x)][1 - P_{\text{outage},R}(x)]. \tag{58}$$

An upper bound of PEP is expressed as [35]

$$\text{PEP}_i(G_1, G_2, \dots, G_K, H_1, H_2, \dots, H_K)$$

$$< P_{\text{outage},e2e,U_i}(W_{TH}) \tag{59}$$

in which W_{TH} is defined in (50).

We deduce the throughput at user U_i :

$$\begin{aligned} \text{Thr}_i(G_1, G_2, \dots, G_K, H_1, H_2, \dots, H_K) &= 0.5 \log_2(Q) \\ &[1 - \text{PEP}_i(G_1, G_2, \dots, G_K, H_1, H_2, \dots, H_K)] \end{aligned} \tag{60}$$

The total throughput is given by

$$\begin{aligned} \text{Thr}(G_1, G_2, \dots, G_K, H_1, H_2, \dots, H_K) \\ = \sum_{i=1}^K \text{Thr}_i(G_1, G_2, \dots, G_K, H_1, H_2, \dots, H_K) \end{aligned} \tag{61}$$

We optimize the fraction of powers allocated to users at the source (H_i) and relay (G_i) to enhance the total throughput

$$\begin{aligned} \text{Thr}^{\max} = \max_{0 < G_1 < G_2 < \dots < G_K < 1, 0 < H_1 < H_2 < \dots < H_K < 1} \\ (G_1, G_2, \dots, G_K, H_1, H_2, \dots, H_K) \end{aligned} \tag{62}$$

under constraints $\sum_{i=1}^K H_i = 1$ and $\sum_{i=1}^K G_i = 1$.

The alternating maximization algorithm [36] was used to maximize the throughput in (62).

4 Theoretical and simulation results

4.1 Single destination

Figures 7, 8, 9 and 10 depict the throughput when RIS is deployed as a reflector to extend the millimeter wave link. These results correspond to fading figure $M = 2$, QPSK, 16QAM, 64 QAM, and 256QAM modulations. Packet length is $L = 400$ symbols. The distance between S and R is $d_4 = 2$. The distance between R and RIS is $d_1 = 1$. The distance between RIS and D is $d_2 = 1$. The path loss exponent is $PLE = 3$. The number of interferers at R is $P = 4$, the number of interferers at D is $Q = 2$ and the average SINR at R is 20 dB. The transmitted energy per symbol of interferers are $E_q = E'_q = 0.01$. Figure 5 shows that RIS allows 19, 25, 31, 37 dB gain with respect to conventional millimeter wave communication without RIS for a number of reflectors $N = 16, 32, 64, 128$. Significant throughput enhancement is observed in Figs. 6, 7 and 8 when RIS is used as a reflector for 16,64 and 256 QAM modulations. Theoretical curves are close to computer simulation results obtained with MATLAB software.

Figures 11 and 12 depict the throughput when RIS is deployed as a transmitter for 8PSK and 16 PSK modulation. The distance between relay and destination is $d_3 = 2.5$ and the other parameter are those of Fig. 7. Figure 11 shows that RIS allows 13, 19, 25, 31 dB gain with respect to conventional millimeter wave communication without RIS for a number of reflectors $N = 16, 32, 64, 128$.

For the same parameters as Fig. 7, Fig. 13 depicts the exact and asymptotic PEP when RIS is used as a reflector for QPSK modulation. To plot the asymptotic PEP, we used equations (26 and 27) and (29–31). At high average SNR, we observe that the asymptotic PEP is close to the exact PEP for a number of reflectors $N = 8, 16, 32$.

The throughput of millimeter wave communications can be improved using antenna selection at the destination [37]. For the same parameters as Fig. 13, Fig. 14 compares the PEP at the destination using RIS to antenna selection. When RIS uses $N = 32, 16, 8$ reflectors, we obtained 26.6, 19.6 and 12.3 dB gain with respect to antenna selection for $n_r = 2$ antennas [37]. When RIS uses $N = 32, 16, 8$ reflectors, we obtained 23.2 16.2 and 8.9 dB gain with respect to antenna selection for $n_r = 3$ antennas [37].

4.2 Results for NOMA systems

We did some simulations using Matlab when there are two NOMA users. The distance between S and R is 1.5 and the distance between R and RIS is 2. The distance between RIS and users are $D_1 = 1, D_2 = 1.5$. The number of interferers at R is $P = 3$. The number of interferers at users is $P_1 = 2, P_2 = 3$. The m-fading figure is $M = 2$.

Figure 15 shows the total throughput for 16QAM modulation, $H_1 = 0.4 = 1 - H_2$ and $G_1 = 0.4 = 1 - G_2$. NOMA system using RIS offers 10,13,16 dB gain with respect to conventional NOMA using millimeter wave communications without RIS [25–28] for a number of reflectors per user $N = N_1 = N_2 = 8, 16, 32$. For an Optimal Power Allocation (OPA), the proposed NOMA using RIS offers 19 dB gain with respect to the absence of RIS [25–28] for a number of reflectors per user $N = N_1 = N_2 = 32$.

Figure 16 depicts the total throughput when there are two NOMA users for 16QAM modulation and $N = N_1 = N_2 = 64, 128, 256, 512$ reflectors per user. The proposed NOMA system using RIS offers 20, 24, 27 and 30 dB gain with respect to conventional NOMA using millimeter wave communications without RIS [25–28] for $N = N_1 = N_2 = 64, 128, 256, 512$.

5 Conclusions and perspectives

In this paper, we suggested extending the coverage of millimeter-wave communications using Reconfigurable Intelligent Surfaces (RIS). The first link between the source and relay node uses millimeter wave communications. In the second link, a RIS is placed between relay node and destination. We suggested implementing RIS as a reflector or a transmitter. The throughput at the destination was derived. Theoretical and simulation results have shown significant throughput enhancement when RIS is implemented as a transmitter or reflector. For QPSK modulation, RIS allows 19, 25, 31, 37 dB gain with respect to conventional millimeter wave communication without RIS for a number of reflectors $N = 16, 32, 64, 128$. We also implemented RIS in mmwave communications using Non Orthogonal Multiple Access (NOMA). Different sets of RIS reflectors are dedicated to the served NOMA users. The proposed NOMA system using RIS offers 10, 13, 16, 20, 24, 27 and 30 dB gain with respect to conventional NOMA using millimeter wave communications without RIS for a number of reflector per user $N = N_1 = N_2 = 8, 16, 32, 64, 128, 256, 512$. One of the limitations of the paper is that the source and relay must have a battery that should be recharged or changed. As a perspective, we can study mmwave using RIS where the source and relay harvest energy using radio frequency signals, solar energy or wind.

Author Contributions The paper is the contribution of Prof. Raed Alhamad and Prof. Hatem Boujemaa.

Funding This publication was supported by Saudi Electronic University.

Data availability Data and material are not available.

Declarations

Conflict of interest The authors state that there is no conflict of interest for this paper.

Appendix A

Let $X = E_S|f|^2$ and $I = \sum_{q=1}^P I_q$. The SNR at R is expressed as $\Gamma_{SR,mmwave} = \frac{X}{I}$. X and I are two independent Gamma r.v. with joint PDF [34]

$$f_{X,I}(x, y) = \frac{x^{M-1}y^{PM-1}e^{-\frac{x}{\beta}}e^{-\frac{y}{\alpha}}}{\Gamma(M)\Gamma(MP)\beta^M\alpha^{MP}} \tag{63}$$

Let $\Gamma_{SR,mmwave} = U = \frac{X}{I}$ and $V = X + I$, the determinant of Jacobian matrix is

$$|J| = \begin{vmatrix} \frac{\partial U}{\partial X} & \frac{\partial U}{\partial I} \\ \frac{\partial V}{\partial X} & \frac{\partial V}{\partial I} \end{vmatrix} = \begin{vmatrix} \frac{1}{I} & -\frac{X}{I^2} \\ 1 & 1 \end{vmatrix} = \frac{X + I}{I^2} = \frac{(1 + U)^2}{V} \tag{64}$$

We can write $I = \frac{V}{1+U}$ and $X = \frac{UV}{1+U}$. We deduce the joint PDF of (U, V)

$$f_{U,V}(u, v) = \frac{f_{X,I}(x, y)}{|J|} = \frac{v}{(1 + u)^2} \left(\frac{v}{1 + u} \right)^{PM-1} \left(\frac{vu}{1 + u} \right)^{M-1} \frac{e^{-\frac{vu}{(1+u)\beta}}e^{-\frac{v}{(1+u)\alpha}}}{\Gamma(M)\Gamma(MP)\beta^M\alpha^{MP}} \tag{65}$$

The PDF of $U = \Gamma_{SR,mmwave}$ is computed as

$$f_U(u) = \int_0^{+\infty} f_{U,V}(u, v)dv. \tag{66}$$

We have [33]

$$\int_0^{+\infty} e^{-Av}v^B dv = \frac{\Gamma(B + 1)}{A^{B+1}} \tag{67}$$

Equations (65–67) give

$$f_{\Gamma_{SR,mmwave}}(u) = \frac{\Gamma(M + PM)\alpha^M u^{M-1}}{\beta^M \Gamma(M)\Gamma(PM)} \left(1 + \frac{u\alpha}{\beta} \right)^{-PM-M} \tag{68}$$

References

1. Zöchmann, E., Groll, H., & Pratschner, S. (2019). A small-scale fading model for overtaking vehicles in a millimeter wave commu-

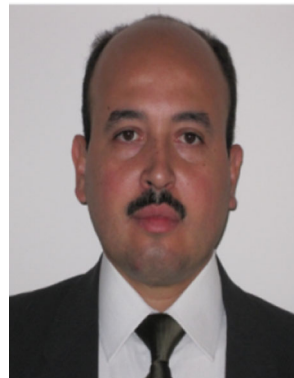
- nication link. In *2019 IEEE 20th international workshop on signal processing advances in wireless communications (SPAWC)*.
2. Jihao, L., Zhenfeng, Y., Yibing, L., Xiaohang, S., Ji, L., & Wei, Z. (2019). Research on millimeter wave phased array antenna for 5G communication. In *2019 IEEE 2nd international conference on electronic information and communication technology (ICEICT)*.
3. Tsai, C.-H., Pepe, F., Mangraviti, G., Zong, Z., Craninckx, J., & Wambacq, P. (2019). A 22.5–27.7-GHz fast-lock bang–bang digital PLL in 28-nm CMOS for millimeter-wave communication with 220-fs RMS jitter. *IEEE Solid-State Circuits Letters*, 2(9), 232–239.
4. Pan, P., Zi, Z., Cai, J., & Feng, J. (2019). Millimeter wave vacuum electronic amplifiers for high data rate communication. In: 2019 44th international conference on infrared, millimeter, and terahertz waves (IRMMW-THz).
5. Kaur, J., & Lal Singh, M. (2019). User assisted cooperative relaying in beamspace massive MIMO NOMA based systems for millimeter wave communications. *China Communications*, 16(6), 103–111.
6. Fukatsu, R., & Sakaguchi, K. (2019). Millimeter-wave V2V communications with cooperative perception for automated driving. In *IEEE 89th vehicular technology conference (VTC2019-Spring)*.
7. Zhang, J., Huang, Y., Xiao, M., Wang, J., & Yang, L. (2018). Energy-efficient cooperative hybrid precoding for millimeter-wave communication networks. In *2018 IEEE global communications conference (GLOBECOM)*.
8. Zhang, J., Huang, Y., Zhang, C., He, S., Xiao, M., & Yang, L. (2017). Cooperative multi-subarray beam training in millimeter wave communication systems. In *GLOBECOM 2017—2017 IEEE global communications conference*.
9. Kaur, J., & Lal Singh, M. (2019). User assisted cooperative relaying in beamspace massive MIMO NOMA based systems for millimeter wave communications. *China Communications*, 16(6), 103–113.
10. Zhu, R., Wang, Y.E., Xu, Q., Liu, Y., & Li, Y.D. (2018). Millimeter-wave to microwave MIMO relays (M4R) for 5G building penetration communications. In *IEEE radio and wireless symposium (RWS), 2018*.
11. Basar, E., Di Renzo, M., De Rosny, J., Debbah, M., Alouini, M.-S., & Zhang, R. (2019). Wireless communications through reconfigurable intelligent surfaces. *IEEE Access*, 7, 116753–116773.
12. Zhang, H., Di, B., Song, L., & Han, Z. (2020). Reconfigurable intelligent surfaces assisted communications with limited phase shifts: How many phase shifts are enough? *IEEE Transactions on Vehicular Technology*, 69(4), 4498–4502.
13. Di Renzo, M. (2019). 6G wireless: Wireless networks empowered by reconfigurable intelligent surfaces. In *2019 25th Asia-Pacific conference on communications (APCC)*.
14. Basar, E. (2020). Reconfigurable intelligent surface-based index modulation: A new beyond MIMO paradigm for 6G. *IEEE Transactions on Communications*, 68, 3187–3196.
15. Wu, Q., & Zhang, R. (2020). Towards smart and reconfigurable environment: Intelligent reflecting surface aided wireless network. *IEEE Communications Magazine*, 58(1), 106–112.
16. Huang, C., Zappone, A., Alexandropoulos, G. C., Debbah, M., & Yuen, C. (2019). Reconfigurable intelligent surfaces for energy efficiency in wireless communication. *IEEE Transactions on Wireless Communications*, 18(8), 4157–4170.
17. Alexandropoulos, G. C., & Vlachos, E. (2020). A hardware architecture for reconfigurable intelligent surfaces with minimal active elements for explicit channel estimation. In *ICASSP 2020—2020 IEEE international conference on acoustics, speech and signal processing (ICASSP)*.
18. Guo, H., Liang, Y.-C., Chen, J., & Larsson, E. G. (2020). Weighted sum-rate maximization for reconfigurable intelligent surface aided wireless networks. *IEEE Transactions on Wireless Communications*, 19, 3064–3076.

19. Thirumavalavan, V. C., & Jayaraman, T. S. (2020). BER analysis of reconfigurable intelligent surface assisted downlink power domain NOMA system. In *2020 international conference on communication systems and networks (COMSNETS)*.
20. Yang, L., Guo, W., & Ansari, I. S. (2020). Mixed dual-hop FSO-RF communication systems through reconfigurable intelligent surface. *IEEE Communications Letters*, *24*, 1558–1562.
21. Di, B., Zhang, H., Li, L., Song, L., Li, Y., & Han, Z. (2020). Practical hybrid beamforming with finite-resolution phase shifters for reconfigurable intelligent surface based multi-user communications. *IEEE Transactions on Vehicular Technology*, *69*(4), 4565–4570.
22. Nadeem, Q.-U.-A., Kammoun, A., Chaaban, A., Debbah, M., & Alouini, M.-S. (2020). Asymptotic max-min SINR analysis of reconfigurable intelligent surface assisted MISO systems. *IEEE Transactions on Wireless Communications*, *19*, 7748–7764.
23. Zhao, W., Wang, G., Atapattu, S., Tsiftsis, T. A., & Tellambura, C. (2020). Is backscatter link stronger than direct link in reconfigurable intelligent surface-assisted system? *IEEE Communications Letters*, *24*, 1342–1346.
24. Dai, L., Wang, B., Wang, M., Yang, X., Tan, J., Bi, S., et al. (2020). Reconfigurable intelligent surface-based wireless communications: Antenna design, prototyping, and experimental results. *IEEE Access*, *8*, 45913–45923.
25. Li, J., Li, X., Ye, N., & Wang, A. (2019). Performance evaluation of MIMO-NOMA in millimeter wave communication for broadcast services. *2019 IEEE international symposium on broadband multimedia systems and broadcasting (BMSB)* (pp. 5–7). Jeju-si: South Korea.
26. Kaur, J., & Singh, M. L. (2019). User assisted cooperative relaying in beamspace massive MIMO NOMA based systems for millimeter wave communications. *China Communications*, *16*(6), 103–113.
27. Guo, L., Cong, S., & Su, C. (2020). On coverage probability of uplink NOMA in millimeter wave cellular networks. In *2020 9th Asia-Pacific conference on antennas and propagation (APCAP)*, 4–7 Aug.
28. Azzahra, M. A. (2019). NOMA signal transmission over millimeter-wave frequency for backbone network in HAPS with MIMO antenna. In *2019 IEEE 13th international conference on telecommunication systems, services, and applications (TSSA)*.
29. Luo, Z., Zhao, L., Tonghui, L., Liu, H., & Zhang, R. (2021). Robust hybrid precoding/combining designs for full-duplex millimeter wave relay systems. *IEEE Transactions on Vehicular Technology*, *70*, 9577–9582.
30. Ma, K., He, D., Sun, H., Wang, Z., & Chen, S. (2021). Deep learning assisted calibrated beam training for millimeter-wave communication systems. *IEEE Transactions on Communications*.
31. Wen, L., Zhiqiang, Y., Zhu, L., & Zhou, J. (2021). High-gain dual-band resonant cavity antenna for 5G millimeter wave communications. *IEEE Antennas and Wireless Propagation Letters*, *20*(10), 1878–1882.
32. Ghasemi, A., & Sousa, E. S. (2007). Fundamental limits of spectrum-sharing in fading environments. *IEEE Transactions on Wireless Communication*, *6*(2), 649–658.
33. Gradshteyn, I. S., & Ryzhik, I. M. (1994). *Table of integrals, series and products* (5th ed.). San Diego, CA: Academic.
34. Proakis, J. (2007). *Digital communications* (5th ed.). New York: Mac Graw-Hill.
35. Xi, Y., Burr, A., Wei, J. B., & Grace, D. (2011). A general upper bound to evaluate packet error rate over quasi-static fading channels. *IEEE Transactions on Wireless Communications*, *10*(5), 1373–1377.
36. Ziskind, I., & Wax, M. (1987). Maximum likelihood estimation via the alternating projection maximization algorithm. *IEEE International Conference on Acoustics, Speech, and Signal Processing, Dallas, Texas*, *12*, 2280–2283.
37. Tan, P., & Nicolas, C. (2021). Millimeter-wave antenna selection switch using advanced CMOS technologies. In *2021 international symposium on electrical and electronics engineering (ISEE)* (pp. 1–4).

Publisher's Note Springer Nature remains neutral with regard to jurisdictional claims in published maps and institutional affiliations.



Raed AlHamad received his B.S. at Information Systems Technology and Minor of Network Security from Southern Illinois University (SIUC), Carbondale, Illinois, in 2009, And the M.Eng. and Ph.D. degrees from Stevens Institute of Technology at Networked Information Systems in 2011 and Electrical Engineering in 2015, respectively. Also, In 2016 he got Edward Peskin Award. Dr. Alhamad has been a faculty member at Saudi Electronic University since 2014. He is an associate professor. His research interests include wireless communications, networking, and cyber security.



Hatem Boujemaa (M'02) was born in Tunis, Tunisia. He received the Engineer's Diploma from "Ecole Polytechnique de Tunis", in 1997, the MSC in digital communications from "Telecom Paris Tech", in 1998 and the Ph. D. degree in electronics and communications from the same university in 2001. From October 1998 to September 2001, he prepared his Ph. D. degree at France Telecom R&D, Issy-les-Moulineaux, France. During this period, he participated in the RNRT project AUBE. From

October 2001 to January 2002, he joined "Ecole Supérieure d'Electricité", Gif-sur-Yvette, France, and worked on mobile localization for RNRT project LUTECE. In February 2002, he joined SUPCOM where he is a Professor. His research activities are in the field of digital communications, DS-CDMA, OFDM and MC-CDMA systems, HARQ protocols, Cooperative Communications, Cognitive radio networks, spectrum sensing, Scheduling, Synchronization, Network planning, Information Theory, Equalization and Antenna Processing.